ELSEVIER

Nuclear Instruments and Methods in Physics Research B 155 (1999) 199–205

NIM B
Beam Interactions with Materials & Atoms

www.elsevier.nl/locate/nimb

Estimation of the information content of medical images produced by scintillators interacting with diagnostic X-ray beams

I. Kandarakis [a], D. Cavouras [a,*], N. Kalivas [b], C.D. Nomicos [c], G.S. Panayiotakis [b]

[a] *Department of Medical Instrumentation Technology, TEI of Athens, Ag. Spyridonos Street, Aigaleo, 12210 Athens, Greece*
[b] *Department of Medical Physics, Medical School, University of Patras, 26500 Patras, Greece*
[c] *Department of Electronics, TEI of Athens, Ag. Spyridonos Street Aigaleo, 12210 Athens, Greece*

Received 29 December 1998; received in revised form 2 March 1999

Abstract

The information content of medical images produced by X-ray beam–scintillator interaction was assessed by a method involving detective quantum efficiency (DQE) and information capacity determination. The method was based on emitted light fluence and modulation transfer function (MTF) measurements and it was employed to evaluate the performance of $(Gd_{0.5}La_{0.5})_2O_2S$:Tb scintillator, which was used in the form of laboratory prepared scintillator screens with coating weights ranging between 20 and 139 mg/cm^2. Screens were excited to luminescence using 80 and 120 kVp X-ray beams. The 83 mg/cm^2 scintillator layer exhibited the highest DQE at zero spatial frequency. Thick scintillator layers displayed higher DQE values in the low frequency range while at high frequencies the DQE of thin scintillators were higher. Additionally, thin scintillator layers showed slow DQE variation with increasing frequency. The information capacity of scintillator layers decreased with increasing coating weight indicating that the information content of images produced by thin scintillating layers is higher and more evenly distributed with respect to spatial frequencies.

1. Introduction

The performance of radiation detectors used in medical imaging systems may be assessed by the amount of diagnostic information displayed in the final image. It has been previously proposed [1–4] that the image information content may be objectively estimated using the concepts of information capacity and signal to noise ratio [2]. The information capacity has been defined [1,3,4] by the relation:

$$C_I = n_P \log_2 N_S, \tag{1}$$

where n_P is the number of images elements (pixels) per unit of area and N_S is the number of distinguishable signal intensity levels that can be registered in an image element. The signal to noise ratio is often described by the detective quantum efficiency (DQE), which has been defined [1] by the ratio:

* Corresponding author. Tel.: +301-9594-558; fax: +301-5910-975; e-mail: cavouras@hol.gr, cavouras@medisp.bme.teiath.gr

0168-583X/99/$ – see front matter
PII: S0168-583X(99)00239-6

$$\mathrm{DQE} = \left[\frac{\mathrm{SNR_O}}{\mathrm{SNR_I}}\right]^2, \tag{2}$$

where $\mathrm{SNR_O}$ is the signal to noise ratio at the output of the imaging system and $\mathrm{SNR_I}$ is the signal to noise ratio at the input of the system.

Information capacity has been conveniently formulated to include signal and noise and has been expressed in terms of SNR and DQE [1,3,4]. Both information capacity and DQE have been defined in the spatial frequency domain in terms of the modulation transfer function (MTF), which expresses the image contrast as a function of spatial frequency as well as the spatial resolution properties of an image receptor.

In the present study, a new approach is developed for the experimental determination of image information content in terms of DQE and information capacity with application to laboratory prepared scintillator layers of $(Gd_{0.5}La_{0.5})_2O_2S$:Tb. The latter is a scintillator mixture exhibiting high performance in a wide range of X-ray energies which, to our knowledge, has never been employed in 50% Gd and 50% La proportions [5].

2. Materials and methods

2.1. Theory

The information capacity (C_I) of an image receptor may be expressed [1,3,4] as a function of the spatial frequency dependent SNR or DQE by the following relations:

$$C_I(Q,w) = \pi \int_0^\infty \times \log_2[1 + \mathrm{SNR_O^2}(Q,u,w)]u\,\mathrm{d}u, \tag{3}$$

or considering (2) as well

$$C_I(Q,w) = \pi \int_0^\infty \log_2[1 + \mathrm{SNR_I^2}(Q,u,w)\mathrm{DQE}(u,w)]u\,\mathrm{d}u, \tag{4}$$

where $\mathrm{SNR_O}$ and $\mathrm{SNR_I}$ denote the output and input signal to noise ratios respectively, Q is the X-ray quantum fluence incident on the scintillator layer of the image receptor, w is the scintillator coating weight and u is the spatial frequency. $\mathrm{SNR_O}$ in Eq. (2) may be evaluated by determining the output signal and quantum noise produced by a scintillator, as follows.

The output signal S_O in the spatial frequency domain may be written as a function of the contrast transfer function (CTF). This function characterizes the spatial frequency dependent response of an imaging system to an input signal [6]:

$$S_O = \bar{\Phi}_L(Q,u,w) = \bar{Q}C_P(Q,u,w), \tag{5}$$

where $\bar{\Phi}_L(Q,u,w)$ is the mean spatial frequency dependent emitted light quantum fluence, $\bar{Q}$ is the mean X-ray quantum fluence averaged over the scintillator area, and C_P denotes the CTF. The latter can be written in terms of MTF [6]

$$C_P(Q,u,w) = \left[\frac{\mathrm{d}\bar{\Phi}_L(Q,w)}{\mathrm{d}Q}\right] M_P(u,w), \tag{6}$$

where $\bar{\Phi}_L(Q,w)$ is the zero spatial frequency emitted light quantum fluence, M_P denotes the MTF and the factor $[\mathrm{d}\bar{\Phi}_L/\mathrm{d}Q]$ is the slope of the scintillator characteristic curve, which describes the conversion from input X-ray quanta into emitted light quanta averaged over the scintillator area. The product of this conversion factor with the mean incident X-ray quantum fluence $\bar{Q}$ gives the mean emitted light quantum fluence at zero spatial frequency $\bar{\Phi}_L(Q,w)$. Thus, Eq. (5) may be written as

$$S_O = \bar{\Phi}_L(Q,u,w) = \bar{\Phi}_L(Q,0,w)M_P(u,w). \tag{7}$$

The output signal to noise ratio may then be expressed as follows:

$$\mathrm{SNR_O}(Q,u,w) = \frac{\bar{\Phi}_L(Q,0,w)M_P(u,w)}{N_Q(Q,u,w)}, \tag{8}$$

where N_Q is a function describing the quantum noise amplitude in the spatial frequency domain. N_Q is equal to the square root of the quantum noise power spectrum (NPS) or Wiener spectrum, which is very often employed in assessing the noise performance of imaging systems.

Using relations (2) and (8), DQE may be expressed as:

$$\mathrm{DQE}(u,w) = \frac{\left[\bar{\Phi}_{\mathrm{L}}(Q,0,w)M_{\mathrm{P}}(u,w)\right]^2}{\bar{Q}W_Q(Q,u,w)} = \frac{\bar{\Phi}_{\mathrm{L}}^2(Q,u,w)}{\bar{Q}W_Q(Q,u,w)}, \quad (9)$$

where W_Q denotes the NPS of the scintillator. The mean incident X-ray quantum fluence $\bar{Q}$ in the denominator of Eq. (9) expresses the input signal to noise ratio squared ($\mathrm{SNR}_{\mathrm{I}}^2$).

The quantum NPS may be expressed [7] by the relation

$$W_Q(Q,u,w) = \bar{\Phi}_{\mathrm{L}}(Q,0,w)\bar{m}_{\mathrm{O}}\bar{g}_{\mathrm{L}}(w)\left[1+\frac{\varepsilon}{\bar{m}_{\mathrm{O}}}\right] \times M_{\mathrm{P}}^2(u,w) + \bar{\Phi}_{\mathrm{L}}(Q,0,w), \quad (10)$$

where $\bar{m}_{\mathrm{O}}$ is the mean number of light quanta created within the scintillator per X-ray quantum absorbed, $\bar{g}_{\mathrm{L}}$ is the mean light transmission efficiency giving the probability for a light quantum to escape the scintillator and ε expresses the excess of the variance in m_{O} with respect to the case that m_{O} follows Poisson distribution [7]. Relation (10) has been obtained by considering that incident X-ray quanta Q follow Poisson statistics while light transmission (g_{L}) as well as X-ray absorption (η_Q) events are binomial processes. Additionally, $Q, m_{\mathrm{O}}, g_{\mathrm{L}}$ and X-ray absorption η_Q were assumed to be independent stochastic variables. It was also considered that there were Q X-ray absorption trials $Q\eta_Q$ optical photon production events and $Q\eta_Q m_{\mathrm{O}}$ light transmission trials [7,10]. The first term of (10) expresses the correlated noise component affected by the various light diffusion processes (scattering, etc.) within the scintillator mass. It has thus been expressed as a product containing the term MTF^2, which describes the influence of light diffusion effects [7].

From relations (3), (4), (9), and (10) and considering Poisson statistics for m_{O} ($\varepsilon = 0$), DQE and information capacity may be written as follows:

$$\mathrm{DQE}(u,w) = \frac{\bar{\Phi}_{\mathrm{L}}(Q,0,w)M_{\mathrm{P}}^2(u,w)}{\bar{Q}\left[\bar{m}_{\mathrm{O}}\bar{g}_{\mathrm{L}}(w)M_{\mathrm{P}}^2(u,w)+1\right]}, \quad (11)$$

$$C_{\mathrm{I}}(Q,w) = \pi\int_0^\infty \log_2\left[1+\frac{\bar{\Phi}_{\mathrm{L}}(Q,0,w)M_{\mathrm{P}}^2(u,w)}{\bar{m}_{\mathrm{O}}\bar{g}_{\mathrm{L}}(w)M_{\mathrm{P}}^2(u,w)+1}\right]u\,\mathrm{d}u, \quad (12)$$

Relations (11) and (12) provide an estimation of the image information content in terms of physical parameters ($\bar{\Phi}_{\mathrm{L}}, m_{\mathrm{O}}, g_{\mathrm{L}}, M_{\mathrm{P}}$), describing the response of a scintillator when interacting with X-ray beams used in medical imaging.

2.2. Implementation

The image information content was assessed in terms of DQE and information capacity as follows:

(1) *Scintillator samples preparation*: Six scintillator layers were prepared from $Gd_2O_2S:Tb$ and $La_2O_2S:Tb$ scintillator powders with mean grain size of approximately 7 μm. The layers were formed by sedimentation of the powders on fused silica substrates as described previously [8–11]. The scintillator coating weights ranged between 20 and 140 mg/cm^2.

(2) $\bar{\Phi}_{\mathrm{L}}$ *determination*: The scintillator was excited to luminescence using 80 and 120 kVp X-ray beams. $\bar{\Phi}_{\mathrm{L}}$ was determined by measuring the light fluence emitted by the scintillator employing an EMI 9558 QB photomultiplier coupled to a Cary 401 electrometer [8–12]. Measurements were performed by following two configurations:

(a) Transmission mode (or front screen configuration), where the light emitted by the non-irradiated scintillator surface was collected. This configuration corresponds to the front screen of a double coated radiographic cassette, to the input screen of an image intensifier, and to other types of detectors (e.g. computed tomography, digital radiography, nuclear medicine).

(b) Reflection mode (or back screen configuration), where the light emitted from the irradiated scintillator surface was collected. This configuration simulates the back screen of a radiographic or mammographic cassettes.

Measurements were corrected by taking into account light losses due to spectral incompatibilities between the scintillator's emission spectrum and the photomultiplier's photosensitivity as well as the light losses due to the geometric incompatibilities between the scintillator and the photomultiplier (distance, active areas, angular distribution of light) [9].

(3) $\bar{Q}$ *determination*: $\bar{Q}$ was determined from exposure measurements. Exposure data were converted into X-ray quantum fluence using the appropriate conversion factor [13]. Values of this factor were obtained from literature [14].

M_P *determination*: M_P was determined by the square wave response function (SWRF) method [9,15,16]. The SWRF was measured by imaging a suitable test pattern (MTF test pattern typ-53 of Nuclear Associates) on a radiographic film (Agfa Curix Ortho GS) by the light of the excited scintillator. The pattern comprised lines of lead of various widths corresponding to spatial frequencies from 0.25 to 10 cycles/mm. In transmission mode measurements, the scintillator layer was sandwiched between the test pattern and the radiographic film while in reflection mode, the film was inserted between the pattern and the scintillator. The SWRF (pattern image) was digitized on a Microtec Scanmaker II SP (1200×1200 dpi) scanner. The MTF was then determined using the digitized SWRF values and Coltman's formula [15,16]:

$$M_P(u,w) = \frac{\pi}{4}\sum_{k=1}^{\infty} b_K \frac{\mathrm{SWRF}[(2k-1)u, w]}{(2k-1)}, \qquad (13)$$

where $b_K = 0$ for $m < n$ and

$$b_K = (-1)^n(-1)^{k-1}, \text{ for } m = n, \qquad (14)$$

n is the number of prime factors other than unity in $(2k-1)$, and m is the number of prime factors other than unity which appear only once in $(2k-1)$ [15].

To obtain the scintillator's MTF, the values obtained by relation Eq. (13) were divided by the scanner and film MTFs, determined by the same method [8].

(5) $\bar{m}_O\bar{g}_L$ (w) *determination*: This product gives the number of emitted light photons per absorbed X-ray quantum, which may be determined by dividing $\bar{\Phi}_L$ by the absorbed fraction of the incident X-ray quantum fluence $\bar{Q}$. This was calculated considering exponential X-ray absorption [9,10], characterized by the X-ray absorption coefficient of $(Gd_{0.5}La_{0.5})_2O_2S$:Tb. The absorption coefficient was determined from data on Gd, La, O, S given by Storm and Israel [14].

3. Results and discussion

Fig. 1 shows the variation of the emitted light quantum fluence per unit of incident X-ray quantum fluence (the ratio $\bar{\Phi}_L$ $(Q,0,w)/\bar{Q}$ in relation (11)) with increasing scintillator coating weight. The data were obtained at 80 and 120 kVp, performing transmission and reflection mode measurements. From the data shown in Fig. 1 the following remarks may be made. (1) The emitted light fluence is higher in reflection mode at both 80 and 120 kVp. This is due to the exponential law of X-ray absorption within the material, which imposes that X-ray energy is mainly absorbed at points close to the irradiated scintillator surface, and hence, light photons are easier transmitted towards that surface. (2) The emitted light fluence is higher at 120 kVp than at 80 kVp in both modes of measurement. This is because of the higher average energy deposited on the scintillator by the absorbed 120 kVp X-rays producing more light quanta. (3) The transmission mode measurements indicate a maximum of light fluence around 75 mg/cm^2 while reflection mode measurements show a plateau of light fluence after 80 mg/cm^2. This is because in transmission measurements, distances traveled by light photons to escape the non-irradiated scintillator side, increase with increasing scintillator thickness. Hence, the proba-

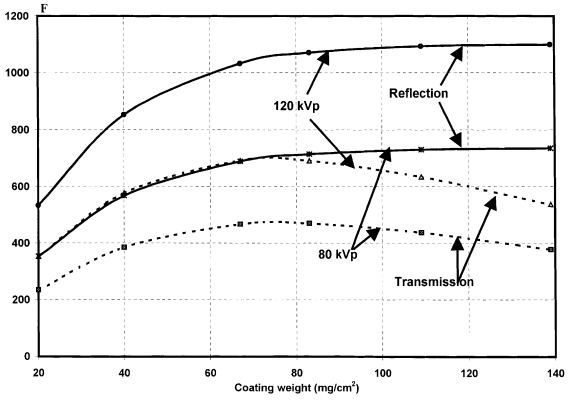

Fig. 1. Variation of the emitted light quantum fluence per unit of incident X-ray quantum fluence (**F**) with increasing scintillator coating weight, measured at 80 and 120 kVp X-ray tube voltages and in both reflection and transmission modes of measurement.

bility of light photon absorption and light fluence attenuation increases resulting in a decrease of Φ_L at thick scintillator layers. On the contrary, in reflection mode, the light photon trajectories do not increase with increasing thickness, since the distances of light creation points from the irradiated side remain practically constant. Thus, reflection mode emission is not considerably affected by the increase in scintillator thickness.

Fig. 2 shows the MTF curves of scintillator layers measured at 80 kVp. As it can be observed, the MTF values of thicker layers are lower; MTF curves drop rapidly with coating weight until 67 mg/cm^2 but slowly thereafter. This happens because MTF depends on the extent of light photon spread during their penetration through a scintillator layer. Light spread is due to the following two effects: (1) Light is isotropically generated within the scintillator material, and thus, laterally directed light photons are spread over a large area at the scintillator's output surface. (2) Light photons are scattered on scintillator grains, and hence, they deviate from their initial direction as they travel through the scintillator material. Both effects increase light spread at the scintillator's emitting surface becoming more significant as thickness increases. This results in an MTF decrease with coating thickness. However, in thick coating weights the lateral light photon trajectories become significantly long, and consequently, the probability of light photon absorption within the scintillator layer mass increases. Thus, in thick scintillator layers the light absorption effects limit the extent of light spread causing slower decrease in MTF.

Fig. 3 shows a comparison of the two MTF curves obtained in transmission and reflection mode measurements. The reflection MTF is clearly higher in the whole spatial frequency range. This difference may be explained by considering that in reflection mode measurements the light photons created within the scintillator layer travel shorter distances both, direct and lateral, to escape from the irradiated scintillator surface. This was also the case in light fluence measurements shown in Fig. 1. This effect restricts the area of light spread at the scintillator's output and improves MTF.

Fig. 4 shows the variation of DQE curves with spatial frequency determined at 80 kVp. At zero spatial frequency, where MTF = 1, the variations of DQE with coating weight was very similar to the corresponding variation of the ratio $\bar{\Phi}_L/\bar{Q}$. The zero frequency DQE was found maximum for the 83 mg/cm^2 layer while the lowest value was found for the 20 mg/cm^2 layer. As spatial frequency increases, the effect of MTF (see relation (11)) causes a more rapid decrease in the DQE of thick layers than in the DQE of thin layers. Thus, the DQE of the 20 mg/cm^2 layer was found highest after the frequency of 80 lp/cm while the 40 mg/cm^2 DQE

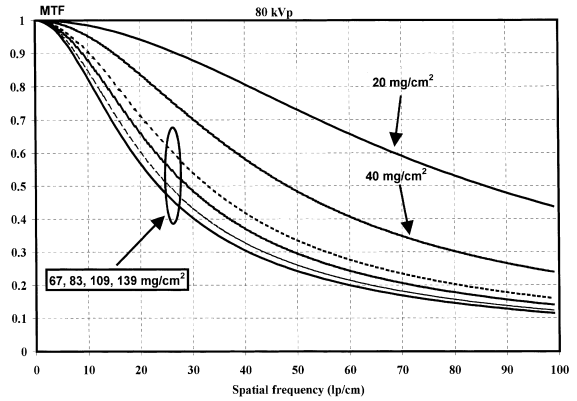

Fig. 2. MTF curves of 20, 40, 67, 83, 109 and 139 mg/cm^2 scintillator layers determined at 80 kVp X-ray tube voltage and in transmission mode of measurement.

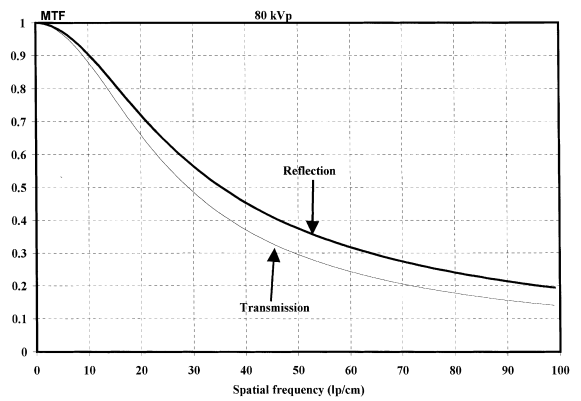

Fig. 3. Comparison of the reflection and transmission mode MTF curves of the 83 mg/cm^2 scintillator layer obtained at 80 kVp X-ray tube voltage.

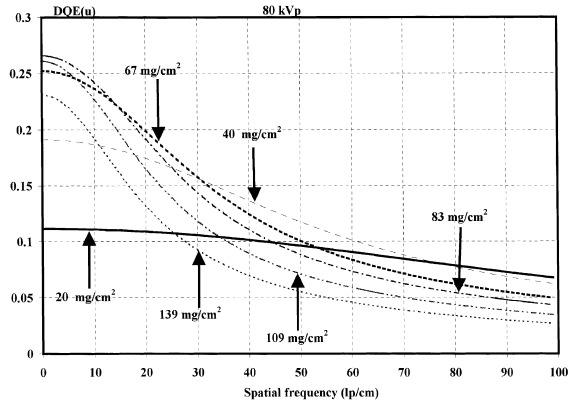

Fig. 4. Spatial frequency dependent DQE curves of the 20, 40, 67, 83, 109 and 139 mg/cm^2 scintillator layers determined at 80 kVp.

was highest in the range between 30 and 80 lp/cm. For the rest of the layers, DQE was inversely proportional to the coating weight in a wide range of spatial frequencies ranging from 15 to 100 lp/cm.

Fig. 5 shows the variation of the information capacity with scintillator coating weight determined in reflection and transmission mode measurements. The values of information capacity are higher in reflection mode and decrease very slightly with increasing thickness especially in the case of reflection mode data. The difference between the two modes of measurements may obviously be attributed to the corresponding differences in the emitted light fluence $\bar{\Phi}_L$ and in MTF. The latter decreases with coating weight and has a tendency to produce similar effect on information capacity values. However, in reflection mode setup, $\bar{\Phi}_L$ increases more or less with increasing scintillator thickness. Thus, the effect of $\bar{\Phi}_L$ counterbalances the influence of MTF, resulting in the slow variation shown in Fig. 4, which is more evident in the curve corresponding to reflection mode. On the other hand, in transmission mode, $\bar{\Phi}_L$ increases up to a limit and decreases slowly thereafter (see Fig. 1). This explains the decline of the transmission mode information capacity curve with respect to the reflection curve at high coating weights.

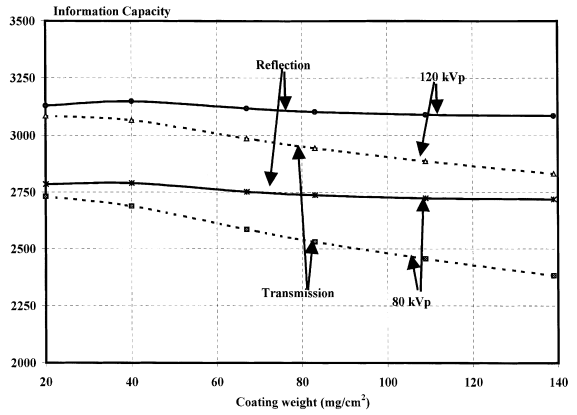

Fig. 5. Variation of the information capacity with increasing scintillator coating weight determined at 80 and 120 kVp X-ray tube voltages in both reflection and transmission modes of measurement.

In conclusion, both image information parameters, DQE and information capacity, depend on the light emission and signal transfer properties $\bar{\Phi}_L$ and M_P which express the quantity and the spatial distribution of the light emitted by the scintillator. DQE is a spatial frequency dependent parameter and is more sensitive to the variation of scintillator thickness while the information capacity is obtained by integration over the spatial frequency domain and is less sensitive to thickness. Additionally, the information capacity depends on the number of incident X-ray quanta ($\bar{Q}$), through $\bar{\Phi}_L$ which is proportional to $\bar{Q}$, while DQE, being proportional to the ratio $\bar{\Phi}_L/\bar{Q}$ is independent of the number of X-ray quanta.

Acknowledgements

This study is dedicated to the memory of Prof. G.E. Giakoumakis, leading member of our team, whose work on scintillator materials has inspired us to continue.

References

[1] J.C. Dainty, R. Shaw, Image Science, Academic Press, London, 1974.
[2] C.E. Dick, J.W. Motz, Med. Phys. 8 (1981) 337.
[3] A.L. Evans, The Evaluation of Medical Images, Adam Hilger Ltd, Bristol, 1981.
[4] H. Kanamori, M. Matsuoto, Phys. Med. Biol. 29 (1984) 303.

[5] H.H. Barret, W. Swindel, Radiological Imaging, Academic Press, New York, 1981.
[6] R. Van Metter, Med. Phys. 19 (1992) 53.
[7] R. Shaw, R. Van Metter, Proc. SPIE 454 (1984) 128.
[8] D. Cavouras, I. Kandarakis, G. Panayiotakis, E.K. Evangelou, C.D. Nomicos, Med. Phys. 23 (1996) 1965.
[9] I. Kandarakis, D. Cavouras, G.S. Panayiotakis, D. Triantis, C.D. Nomicos, Nucl. Instr. and Meth. A 399 (1997) 335.
[10] I. Kandarakis, D. Cavouras, E. Kanellopoulos, G.S. Panayiotakis, C.D. Nomicos, Nucl. Instr. and Meth. A 417 (1998) 86.
[11] I. Kandarakis, D. Cavouras, E. Kanellopoulos, C.D. Nomicos, G.S. Panayiotakis, Med. Biol. Eng. Comput. 37 (1999) 25.
[12] G.W. Ludwig, J. Electrochem. Soc. 118 (1971) 1152.
[13] W.R. Hendee, Medical Radiation Physics, Year Book Medical Publishers, Chicago, 1970.
[14] E. Storm, H. Israel, Photon cross-sections from 0.001 to 100 MeV for elements 1 through 100, Report LA-3753, Los Alamos Scientific Laboratory of the University of California, 1967.
[15] ICRU, Modulation transfer function of screen-film systems, ICRU Report 41, 1986.
[16] G.T. Barnes, The Physics of Medical Imaging: Recording System, Measurements and Techniques, American Association of Physicists in Medicine, New York, 1979.